ELSEVIER

Journal of Hazardous Materials B96 (2003) 259–276

Journal of Hazardous Materials

www.elsevier.com/locate/jhazmat

Treatment of brines by combined Fenton's reagent–aerobic biodegradation II. Process modelling

Francisco J. Rivas*, Fernando J. Beltrán, Olga Gimeno, Pedro Alvarez

Departamento de Ingeniería Química y Energética, Universidad de Extremadura, Avenida de Elvas S/N, Badajoz 06071, Spain

Received 19 July 2001; received in revised form 10 February 2002; accepted 28 July 2002

Abstract

Process modelling of the integrated Fenton's reagent–aerobic biodegradation system has been carried out by considering a detailed reaction mechanism for the chemical oxidation step and the generalised Monod equation for the biological treatment. Chemical oxygen demand has been contemplated as a pseudo-component for simulation purposes. The proposed mechanism takes into consideration different features experimentally found. Thus, the inefficient hydrogen peroxide decomposition into oxygen and water, the influence of temperature and other operating variables and the role of oxygen have been considered. The aerobic biodegradation of the effluent after the chemical oxidation has taken place has been well simulated by Monod equation with no inhibitory terms. Dependency on temperature has been correlated by Arrhenius expression.
© 2002 Elsevier Science B.V. All rights reserved.

Keywords: Brines; Fenton's reagent; Aerobic biodegradation; Table olive wastewater; Modelling

1. Introduction

The presence of significant amounts of chloride in a number of industrial effluents involves an additional difficulty to effectively treat this type of wastewater. Thus, some food-stuff related processes generate effluents characterised not only by a high saline content but also by an important organic load with a variety of contaminants.

Biological methods are by far the most used technology, however, in some cases important drawbacks may dissuade its direct application with sufficient effectiveness outlook. Thus,

* Corresponding author. Tel.: +34-924-289385; fax: +34-924-271304.
E-mail address: fjrivas@unex.es (F.J. Rivas).

0304-3894/03/$ – see front matter © 2002 Elsevier Science B.V. All rights reserved.
PII: S0304-3894(02)00216-9

effluents containing high levels of toxic or refractory substances towards microorganisms are not suitable to be treated by conventional bioprocesses. Heavy metals, phenolic-type compounds, high concentration of salts, organics, etc. might inhibit the aerobic (or anaerobic) action of the biomass. Also, variations in the main characteristics of the wastewater may deteriorate the biological wastewater plant performance. Chemical oxidation might provide a suitable alternative to conventional treatments when dealing with problematic effluents.

Inspite of the presence of high Cl^- concentration, Fenton's reagent (a mixture of hydrogen peroxide and ferrous or ferric iron) has been demonstrated to be a feasible technology to reduce the organic content of brines from table olive manufacturing processes. Hence, in a previous paper, chemical oxygen demand (COD) conversions in the interval 80–90% have been reported [1].

Fenton's reagent was discovered more than 100 years ago. Since then, numerous studies have dealt with the oxidation of either model compounds and real effluents. In this technology, the ferrous and/or ferric cation catalytically decomposes the hydrogen peroxide to generate powerful oxidising agents [2–4] able to degrade a number of organic and inorganic substances. Fenton's reagent is a complicated system that involves a large number of reactions including red-ox reactions, complexation, precipitation equilibrium, etc. Modelling of Fenton's systems is not an easy task even when using model compounds dissolved in ultrapure water. An additional difficulty arises from the uncertainty in the nature of the oxidising species generated during the process. Two main theories have been developed and reported in the past and recent literature. The first one is based on the formation of radical species to initiate a radical chain mechanism [5]. The second one postulates the generation and existence of aquo or organocomplexes of high valence iron, for instance the ferryl or perferryl ion [6].

Consequently, few works have been focused on the proposal and development of detailed reaction mechanism. Nevertheless, some authors have faced mechanistic studies on the kinetics of pure compounds. Thus, Chen and Pignatello investigated the influence of some organic reductants in the oxidation of phenol [7]. Also Rivas et al., based on the former authors, studied the degradation of *p*-hydroxybenzoic acid by continuous feeding of Fenton's reagent constituents [8]. Other works reported in the literature have been addressed to bring to light specific features of the Fenton treatment. Moreover, particular attention has been paid to clarify the nature of the oxidising agent involved in the process, to elucidate the limiting–initiating steps, to assess the role of some organic and/or inorganic species, etc. [9,10].

Strikingly, although Fenton wastewater remediation has been considered from the late 1960s, few attempts have been made to apply the knowledge in this field to the modelling of real effluent treatments. Therefore, simple power kinetics have been used to describe the contamination reduction achieved when processing industrial wastewaters.

In this work, a first attempt has been carried out to simulate the performance of the Fe(II)/Fe(III)/H_2O_2 system when treating wastewater from the production of table olives (fermentation brines). Obviously, the proposed model can not account for the whole group of reactions that actually might occur. However, the model may represent a first step to understand and gain an insight of the different behaviours observed in the treatment of industrial aqueous residues. In addition, the aerobic biodegradation of the effluent after the chemical oxidation has been modelled by using acclimated seeds.

2. Materials and methods

Chemical oxidation experiments were carried out in a 500 ml stirred glass reactor under sunlight conditions, batchwise and (unless otherwise specified) in the presence of oxygen. Systematically, samples were withdrawn and immediately analysed after sampling (in less than 2 min).

Fermentation brines were taken from a factory located in Navalvillar de Pela in the province of Badajoz (Southwest of Spain). Most of experiments were carried out after dilution of the raw wastewater with synthetic urban wastewater with a dilution factor of 2 (one part brines + one part synthetic urban wastewater).

All chemicals were provided by Aldrich and used without further purification. Analysis of chemical oxygen demand (COD) was determined in a Dr. Lange spectrophotometer, the method based on the dichromat standard procedure. Total peroxides concentration was determined iodometrically. Ferrous ion in the solution was analysed by the 2,4,6-tripyridyl-s-triazine (TPTZ) method, this analysis was carried out after hydrogen peroxide removal through decomposition with catalase. Details of the analytical procedure can be found elsewhere [1]. The pH of the reaction media was followed by means of a Radiometer Copenhagen pH-meter (HPM82).

Biodegradation of fermentation brines was carried out in a 500 ml glass sequencing batch reactor (SBR) containing a given amount of suspended activated sludge. Control analysis was conducted on the SBR for temperature, pH and dissolved oxygen. During the reaction period, samples of the mixed liquor were steadily withdrawn and centrifuged. The liquid and solid phases thus obtained were analysed for volatile suspended solids (VSS) and chemical oxygen demand (COD), respectively.

In biodegradation experiments biomass concentration was related to the concentration of VSS.

3. Results and discussion

3.1. Mechanism proposal—general considerations

At the sight of experimental results obtained in the Fenton's treatment of fermentation brines, the following considerations might be proposed:

- The wide spectrum of substances present in this type of wastewater makes non-viable the development of a rigorous kinetic model by individually taking into account each group of compounds. As a consequence, the COD of the effluent has been considered as a pseudo-component subject to oxidation.
- As stated previously, the nature of the oxidant generated during the process is unclear. Whatever the case, the similarities in reactivity between the hydroxyl radical (classic mechanism) and high valence forms of iron [10,11] have been reported. Moreover, some authors have postulated the co-existence of both species depending on operating conditions [12,13]. For simplicity purposes, in this work, the classic Fenton's mechanism to form the hydroxyl radical has been assumed to initiate the oxidation.

- The presence of significant amounts of phenol-type substances (>1000 ppm) suggests the existence of a red-ox cycle of the ferric and ferrous cations. Some of these substances (i.e. gallic acid) have been reported to be capable of reducing Fe(III) to Fe(II) in the presence or absence of light [14]. In addition, some typical intermediates in phenol-like species oxidation (quinones) and some organic radicals (semi-quinone radical, cyclohexadienyl radical, etc.) are also capable of exchanging an electron to transform Fe(II) into Fe(III) [7,8,15].
- The inevitable formation of organic and inorganic iron complexes complicates even more the resolution of the modelling problem [16]. The reactivity of these complexes towards H_2O_2 may be affected depending on the chelating agent nature [17]. Thus, carboxylic acids are known to accelerate the reaction between iron and hydrogen peroxide [18]. Contrarily, other ligands (i.e. phosphates) inhibit the oxidation by stabilising the cation and by scavenging the radicals formed during the process, therefore preventing the organic matter of being oxidised [19]. For the particular case of brines the content in chloride has to be necessarily accounted for. The influence of Cl^- in advanced oxidation processes (AOPs) has been recently investigated [20,21].
- From experimental results, it was noticed a rapid conversion of H_2O_2 (>95%) at the beginning of the reaction ($C_{Fe(III)}$> 0.01 M; $C_{H_2O_2} = 1.0$ M) with a significant release of oxygen. At the sight of the classic Fenton's mechanism, the drastic initial decomposition of H_2O_2 would result in the disappearance of the oxidant source (i.e. hydroxyl radical) and hence, the end of the oxidation reaction. However, COD removal progressed for the entire period of the experiments suggesting the development of parallel routes of COD elimination. In this sense, formation of organic radicals capable of propagating the radical mechanism by combination with oxygen has been previously postulated [9,22]. Moreover, Utset et al. [23] have reported the partial replacement of H_2O_2 by O_2 as electron acceptors in Fenton and photo-Fenton reactions of aniline.
- Taken into account the influence of variables shown in the previous paper, it is observed a Fe(III) concentration level (>0.01 M) above which, a notorious increase in H_2O_2 decomposition rate is noticed. These results may suggest a shift in the reaction mechanism, predominating different routes of oxidation depending on the ratio H_2O_2/Fe(III). Thus, Tung et al. [24] claimed that the metal:peroxide ratio was decisive with respect to reactivity and product profile in Fenton-like systems. Additionally, other authors have hypothesised that the nature of the predominant radical varies depending on operating conditions (i.e. pH) and the excess of H_2O_2 over iron species [10,13].

3.2. Mechanism

In view of the previous comments, the following set of reactions was therefore proposed:

$$Fe^{2+} + H_2O_2 \rightarrow Fe^{3+} + OH^- + HO^\bullet \quad (k_{i2}) \tag{1}$$

$$Fe^{3+} + H_2O_2 \rightarrow Fe^{2+} + H^+ + HO_2^\bullet \quad (k_{i3}) \tag{2}$$

$$H_2O_2 + HO^\bullet \rightarrow HO_2^\bullet + H_2O \quad (k_{p1} = 2.7 \times 10^7) \tag{3}$$

$$Fe^{2+} + HO^\bullet \rightarrow Fe^{3+} + OH^- \quad (k_{p2} = 4.3 \times 10^8) \tag{4}$$

$$Fe^{3+} + HO_2^{\bullet} \rightarrow Fe^{2+} + O_2 + H^+ \quad (k_{r1} = 10^4) \tag{5}$$

$$Fe^{2+} + HO_2^{\bullet} + H^+ \rightarrow Fe^{3+} + H_2O_2 \quad (k_{01} = 1.2 \times 10^6) \tag{6}$$

$$Fe^{3+} + {}^{\bullet}O_2^- \rightarrow Fe^{2+} + O_2 \quad (k_{r2} = 1.5 \times 10^8) \tag{7}$$

$$Fe^{2+} + {}^{\bullet}O_2^- + 2H^+ \rightarrow Fe^{3+} + H_2O_2 \quad (k_{02} = 10^7) \tag{8}$$

$$COD + HO^{\bullet} \rightarrow COD^{\bullet} + H_2O \quad (k_{OH} = 5.0 \times 10^9) \tag{9}$$

$$COD^{\bullet} + O_2 \rightarrow CODO_2^{\bullet} + H_2O \quad (k_{p3} = 1.0 \times 10^9) \tag{10}$$

$$CODO_2^{\bullet} + COD \rightarrow CODO_2H + P \quad (k_{perox} = 1.0 \times 10^6) \tag{11}$$

$$CODO_2H \overset{\Delta H/\text{catalyst}}{\rightarrow} HO^{\bullet} + P \quad (k_{i4}) \tag{12}$$

$$H_2O_2 \overset{\Delta H/\text{catalyst}}{\rightarrow} \tfrac{1}{2}O_2 + H_2O \quad (k_{\text{ineff}}) \tag{13}$$

$$Fe^{3+} + COD^{\bullet} \rightarrow Fe^{2+} + P + H^+ \quad (k_{r3} = 1.0 \times 10^5) \tag{14}$$

$$Cl^- + OH^{\bullet} \leftrightarrows ClOH^{\bullet -} \quad (k_{Cl1} = 4.3 \times 10^9 / k_{Cl1} = 6.1 \times 10^9) \tag{15}$$

$$ClOH^{\bullet -} + H^+ \rightarrow Cl^{\bullet} + H_2O \quad (k_{Cl2} = 4.3 \times 10^8) \tag{16}$$

$$Cl^{\bullet} + H_2O_2 \rightarrow H^+ + Cl^- + HO_2^{\bullet} \quad (k_{Cl3} = 1.0 \times 10^9) \tag{17}$$

$$Cl^{\bullet} + Fe^{2+} \rightarrow Fe^{3+} + Cl^- \quad (k_{Cl4} = 6.0 \times 10^9) \tag{18}$$

$$2HO_2^{\bullet} \rightarrow H_2O_2 + O_2 \quad (k_{T1} = 8.3 \times 10^5) \tag{19}$$

$$2HO^{\bullet} \rightarrow H_2O_2 \quad (k_{T2} = 5.2 \times 10^9) \tag{20}$$

$$HO_2^{\bullet} \leftrightarrows {}^{\bullet}O_2^- + H^+ \quad (K_{\text{equil}} = 8 \times 10^5) \tag{21}$$

Units in mole, liter and second. References for rate constants: [7,8,20].

Obviously, the set of reactions (1)–(21) is far from accounting for all the possible reactions occurring in the actual process. Thus, other species which could play a significant role in the overall mechanism are: $RO^{\bullet}$, $Cl_2^{\bullet -}$, etc. However, it results quite difficult to evaluate the influence of all these species. Albeit, it is believed that the most important reactions potentially occurring in the media have been taken into consideration.

In any case, some assumptions made on the above model have to be clarified. The following points have been considered:

- The value of k_{OH} has been fixed in the range 10^9 to $10^{10}\,M^{-1}s^{-1}$. This is the typical order of magnitude of k_{OH} with most of organic compounds [25].
- The value of kinetic constants for the combination of molecular oxygen with organic radicals have been compiled by Neta et al. [26]. These authors have reported values in the proximity of $10^9\,M^{-1}\,s^{-1}$ for this type of reactions. Therefore, k_{p3} has been given a similar value.

- Also, in the aforementioned study [26], some values of the reaction rate between organic peroxyl radicals and molecular compounds to form the corresponding peroxide are shown. The kinetics of this type of reactions strongly depends on the nature of both the peroxyl radical and the organic molecule. Broadly speaking, the reactivity of alkylperoxyl radicals is lower than the corresponding substituted radicals. Regarding the nature of the organic substrate to be oxidised, values in the interval 10^4 to $10^8\,M^{-1}\,s^{-1}$ are reported for chemical families with aromatic structure (hydroquinone, phenol, phenolate, etc.) or carboxylic acids of high molecular weight (linoleic, linolenic, oleic, etc.). Both types of substances are found in these effluents in relatively high proportion. Hence, an average value of K_{perox} has been assumed ($K_{perox} = 10^6\,M^{-1}\,s^{-1}$).
- The rate constant values k_{i2}, k_{i3}, k_{i4} and k_{ineff} are, a priori, difficult to be evaluated. The values of k_{i2} and k_{i3} are affected by the presence of chelators able to stabilise the cation slowing down the reaction or, contrarily, activate and accelerate the reaction [16,17]. Also, the heterogeneous catalytic decomposition (on solid surfaces) of peroxides may play an important role in the evolution of the system [27]. Formation of a whitish precipitate was observed when the Fe(III) initial concentration was above 0.01 M. Thus, breakage of the hydrogen peroxide against the reactor walls or the surface precipitate may lead, to some extent, to an inefficient use of this reagent to finally yield oxygen and water [24] or to the less reactive hydroperoxide radical [28].
- As discussed later in the paper, the value of k_{i2} is unimportant since this is not a controlling step. Contrarily, k_{i3}, k_{i4} and k_{ineff} are key reactions and their values should be calculated for each particular system and effluent type [8].
- Finally, the reaction rate value for the reduction of ferric iron to ferrous iron by organic radicals have been assumed in the range 10^4 to $10^5\,M^{-1}\,s^{-1}$. This order of magnitude for k_{r3} has already been used for the reaction of aromatic radicals with ferric iron [8]. For instance, Chen and Pignatello [7] calculated a value of $4.4 \times 10^4\,M^{-1}\,s^{-1}$ for the reduction of ferric iron by means of the dihydrocyclohexadienyl radical. In this work, a generic value of $10^5\,M^{-1}\,s^{-1}$ has been given.

3.3. Modelling experimental results

The system of first order differential equations derived from reactions (1)–(21) for a perfectly mixed batch reactor was numerically solved by using a mathematic algorithm based on the evolutionary programming (EP) method [29]. This method is a computational technique that mimics evolution and is based on reproduction and selection [30]. Optimization was carried out by using the method of Jevenberg–Mardquardt.

Fig. 1 shows the experimental and computed results for the Fenton oxidation of table olive fermentation brines carried out at different temperature with an initial Fe(III) and H_2O_2 concentrations of 0.03 and 1.0 M, respectively. As observed from this figure, the model acceptably simulates the evolution of both parameters throughout the whole reaction period. Also, the numeric resolution of the differential equations allowed for the calculation of other species generated in the process. In Fig. 2 (A) the evolution of organic peroxides and ferrous iron is plotted against the reaction time. Given the complexity of the system studied in this work, it can be said that the proposed mechanism does a good job in fitting the evolution of ferrous iron (organic peroxides were not measured in this work). It is noticed

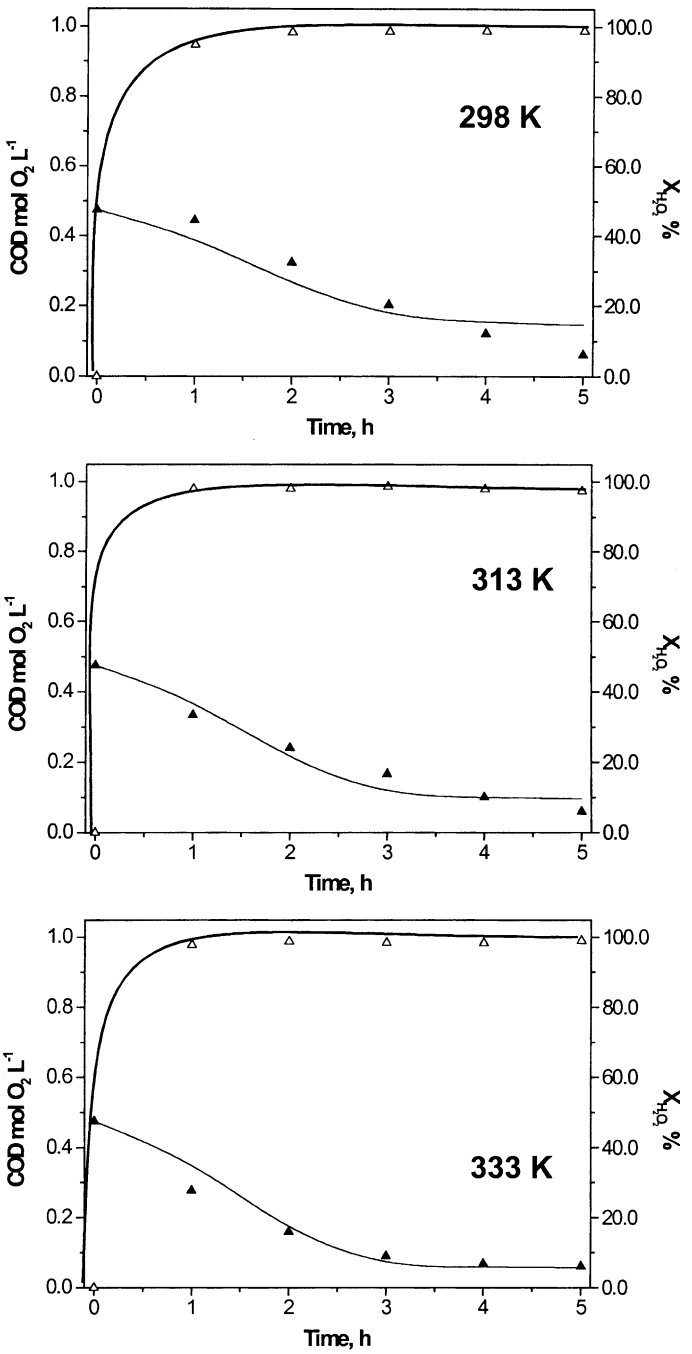

Fig. 1. Fe(III)/H_2O_2 treatment of fermentation table olive brines. Evolution of COD (solid symbols) remaining concentration and H_2O_2 conversion (open symbols) with time. Influence of temperature. Conditions: $pH_o = 3.5$; $C_{H_2O_2} = 1.0\,M$; $C_{Fe(III)} = 0.03\,M$; $C_{COD_o} = 15\,g\,l^{-1}$ (average value). Symbols: experimental results. Lines: model calculations.

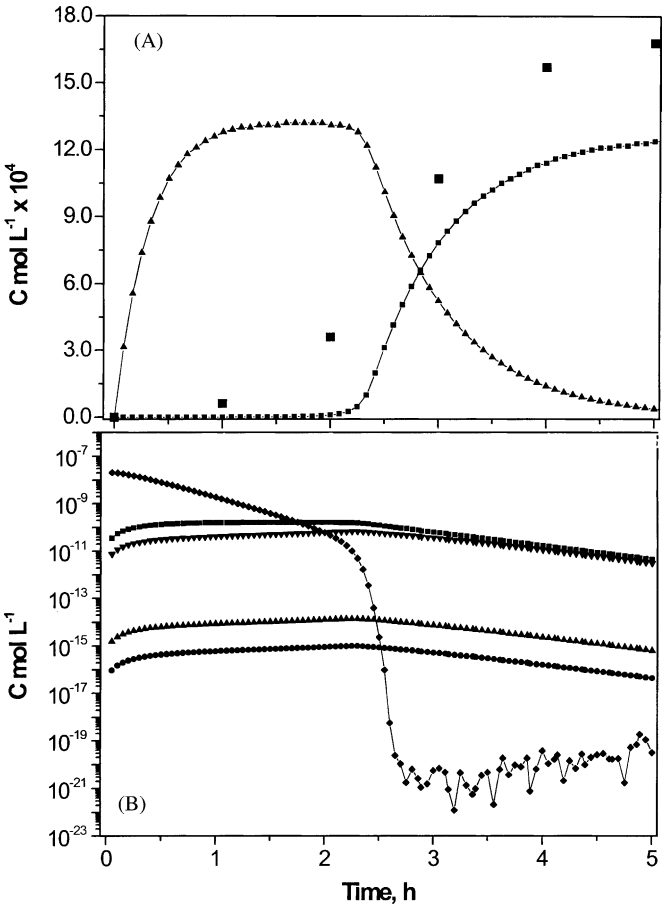

Fig. 2. Fe(III)/H_2O_2 treatment of fermentation table olive brines. Conditions: pH_o = 3.5; T = 298 K; $C_{H_2O_2}$ = 1.0 M; $C_{Fe(III)}$ = 0.03 M; C_{COD_o} = 15 g l^{-1} (average value). (A) Computed evolution of organic peroxides (▲) $CODO_2H$ and (■) Fe(II) concentrations with time. Symbols: experimental results. Lines + small symbols: model calculations. (B) Computed evolution of radical concentrations with time. (◆) $HO_2^{\bullet}$, (■) $COD^{\bullet}$, (▼) $CODO_2^{\bullet}$, (▲) $HO^{\bullet}$ and (●) $Cl^{\bullet}$.

that ROOH and Fe(II) do follow an opposite behaviour with the accumulation of the latter as peroxides disappear from the media. Effectively, after a significant decrease of COD in the first 3 h of reaction, ferric iron reduction steps predominate (mainly reaction (14)) over the stages (10) and (11).

Fig. 2 (B) shows the concentration profiles of the radical species considered in this study. From this plot, it is deduced that with the exception of hydroperoxide radicals, the hypothesis of steady state may be assumed for the rest of radicals. Concentration values typically found in the literature for this type of species were, therefore, obtained (i.e. $C_{HO^{\bullet}} = 10^{-15}$ to 10^{-13} M).

For the conditions used in this work, and among the adjustable parameters in this mechanism, strikingly, only k_{i4} was sensitive to variations in temperature. Nevertheless, as stated previously, rate constant values were numerically obtained, and consequently, they should be taken with caution. The other two fitted parameters k_{ineff} and k_{i3} took values of $9.0 \pm 0.3 \times 10^{-4}\,s^{-1}$ and $2 \pm 0.5 \times 10^{-5}\,M^{-1}\,s^{-1}$, respectively. Additionally, an Arrhenius plot of k_{i4} numerically calculated at different temperatures allowed for the following expression: $\ln(k_{i4}) = -0.788$ to $1073/T$ ($R^2 = 0.99$).

Given the values of k_{ineff} and k_{i3}, it can be observed how the inefficient decomposition of hydrogen peroxide practically consumes this reagent at the first stage of the process. The ratio for both routes can be approximately calculated as $k_{ineff}/(Fe^{3+}\ k_{i3}) \approx 10^{-3}/(0.03 \times 2 \times 10^{-5}) \approx 2 \times 10^{3}$ indicating the wastage of H_2O_2. It has to be mentioned the low value of k_{i3} if compared to reported values in pure water. This may indicate that Fe^{3+} is stabilized by complexation, however this assumption is speculative in nature since, as reminded before, rate constants have been obtained by a numerical method and should be taken as a mere indication of the significance of a specific step in the mechanism. Unfortunately, as commented previously in Section 1, there are not many models in the literature dealing with real wastewaters and comparison of calculated parameters is not possible.

3.4. Validation of the kinetic model

3.4.1. Influence of dissolved oxygen

At the sight of the proposed model and calculated parameters, it can be inferred that the presence of oxygen in the reaction media is of paramount importance when the Fe(III) initial concentration is high (>0.01 M). Therefore, the concentration of O_2 should play, a priori, an important role in the performance of the oxidation and elimination of COD. The latter statement is adequately predicted by the model. Thus, in Fig. 3 (A) it is observed the positive influence exerted by this parameter in the COD final conversion, when oxygen concentration is increased from 10^{-5} to 5×10^{-4} M. In order to ascertain the predictions inferred from the model, an experiment was carried out by continuously bubbling helium through the reaction matrix. Therefore, oxygen concentration was decreased up to a value of approximately 10^{-5} M during the experiment. As observed from Fig. 3 (B), the theoretical predictions were acceptably confirmed by the kinetic mechanism. Discrepancies between experimental and computed results might be explained based on the non-isothermal character of the experiment completed (not considered by the mechanism), and also on the variability in oxygen concentration observed during the experiment. In any case, the theoretical results obtained are relatively surprising since it is observed the disappearance of the inhibition period under conditions of oxygen shortage, albeit at the end of the reaction, the model predicts similar COD conversion values to those experimentally obtained.

3.4.2. Influence of the initial Fe(III) concentration

As reported previously, Fe(III) concentrations below 0.02 M ($C_{H_2O_2} = 1.0$ M) lead to an important decrease in hydrogen peroxide decomposition rate. For instance, if the ferric concentration is set at 0.005 M, H_2O_2 can be measured at significant concentrations for the whole reaction period (5–6 h).

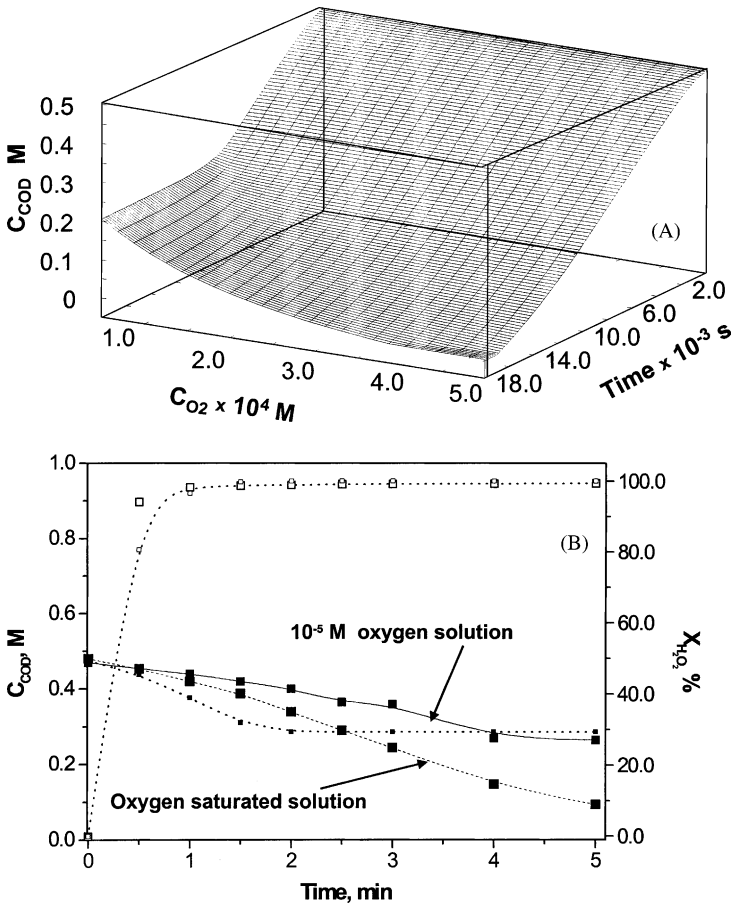

Fig. 3. Fe(III)/H_2O_2 treatment of fermentation table olive brines. Influence of oxygen concentration. Conditions: $pH_o = 3.5$; $T_o = 298$ K; $C_{H_2O_2} = 1.0$ M; $C_{Fe(III)} = 0.03$ M; $C_{COD_o} = 15\,g\,l^{-1}$ (average value). (A) Model simulation. (B) Evolution of COD remaining concentration and H_2O_2 conversion with time. (■) COD. Solid line: oxygen concentration $\approx 10^{-5}$ M, dashed line: oxygen saturated solution, (❑) H_2O_2. Dotted lines + small symbols: model calculations for oxygen concentration $= 10^{-5}$ M.

Hence, the kinetic mechanism used for high Fe(III) concentrations was tested for lower amounts of this reagent. Although, experiments for Fe(III) below 0.03 M were conducted with no temperature control and, therefore, direct comparison with computed results is not correct, the model failed when lowering the value of this parameter. Thus, predicted COD conversion drastically diminished meanwhile H_2O_2 disappeared with similar rates to that observed for the higher Fe(III) concentrations. These results suggest that in the proposed mechanism, k_{ineff}, which is a pseudo-empirical constant, may depend on ferric iron initial concentration, determining its value the main route for hydrogen peroxide decomposition. Consequently, the lower k_{ineff} the higher the importance of H_2O_2 removal through reaction (2). In Fig. 4, it can be observed the fitted results obtained for an experiment carried out with initial Fe(III) $= 0.005$ M. In this case, k_{ineff} calculated by the model was $1.5 \times$

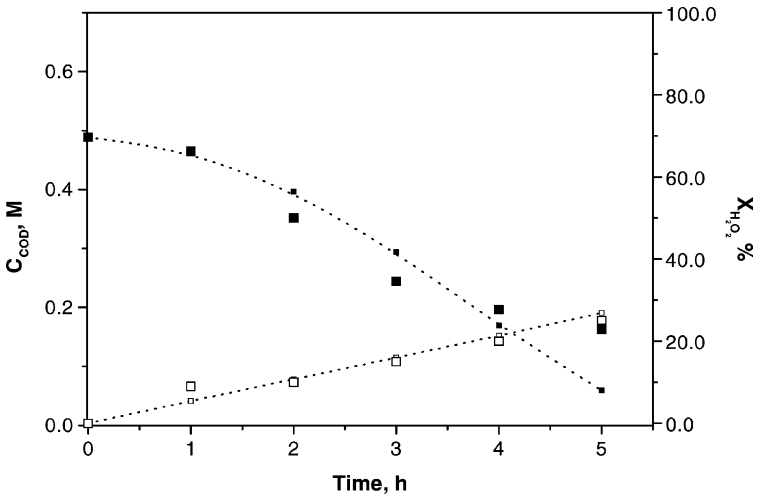

Fig. 4. Fe(III)/H_2O_2 treatment of fermentation table olive brines. Evolution of COD remaining concentration and H_2O_2 conversion with time. Conditions: $pH_o = 3.5$; $T_o = 98$ K; $C_{H_2O_2} = 1.0$ M; $C_{Fe(III)} = 0.005$ M; $C_{COD_o} = 15\,g\,l^{-1}$ (average value). Symbols: experimental results. Lines: model calculations.

$10^{-5}\,s^{-1}$, keeping constant the rest of reaction rates. Similar values for this parameter have already been reported for the Fenton's treatment of olive oil mill wastewater [4]. Given the dependency of k_{ineff} on the initial Fe(III), some more work has to be done to establish a suitable correlation between both parameters at isothermal conditions.

3.5. Sensitivity analysis of the kinetic model

3.5.1. Kinetic constant COD-hydroxyl radical, k_{OH}

The evolution of COD (see Fig. 5 (A)) and H_2O_2 with time were theoretically calculated for values of k_{OH} in the interval 5×10^7 to $10^{11}\,M^{-1}\,s^{-1}$. This rate constant slightly affected the process for values abnormally low (5×10^7 to $10^8\,M^{-1}\,s^{-1}$). Values above $10^8\,M^{-1}\,s^{-1}$ did not influence the efficiency of the process.

3.5.2. Kinetic constant for the formation of the organoperoxyl radical, k_{p3}

The value of k_{p3} was tested in the interval 5×10^7 to $5 \times 10^{10}\,M^{-1}\,s^{-1}$. As inferred from Fig. 5 (B) a slight increase of the final COD conversion is obtained as far as the value of k_{p3} approaches $5 \times 10^8\,M^{-1}\,s^{-1}$. From this point, no influence was observed.

3.5.3. Kinetic constant COD—organoperoxyl radical, k_{perox}

No influence of k_{perox} was observed in the interval 5×10^4 to $5 \times 10^8\,M^{-1}\,s^{-1}$.

3.5.4. Kinetic constant for organoperoxide decomposition, k_{i4}

This constant was numerically determined by fitting experimental and computed results. To check for the influence of this rate constant in the mechanism of reactions, values in the range 0.005–0.05 s^{-1} were given. Fig. 5 (C) shows the computed COD evolution with time

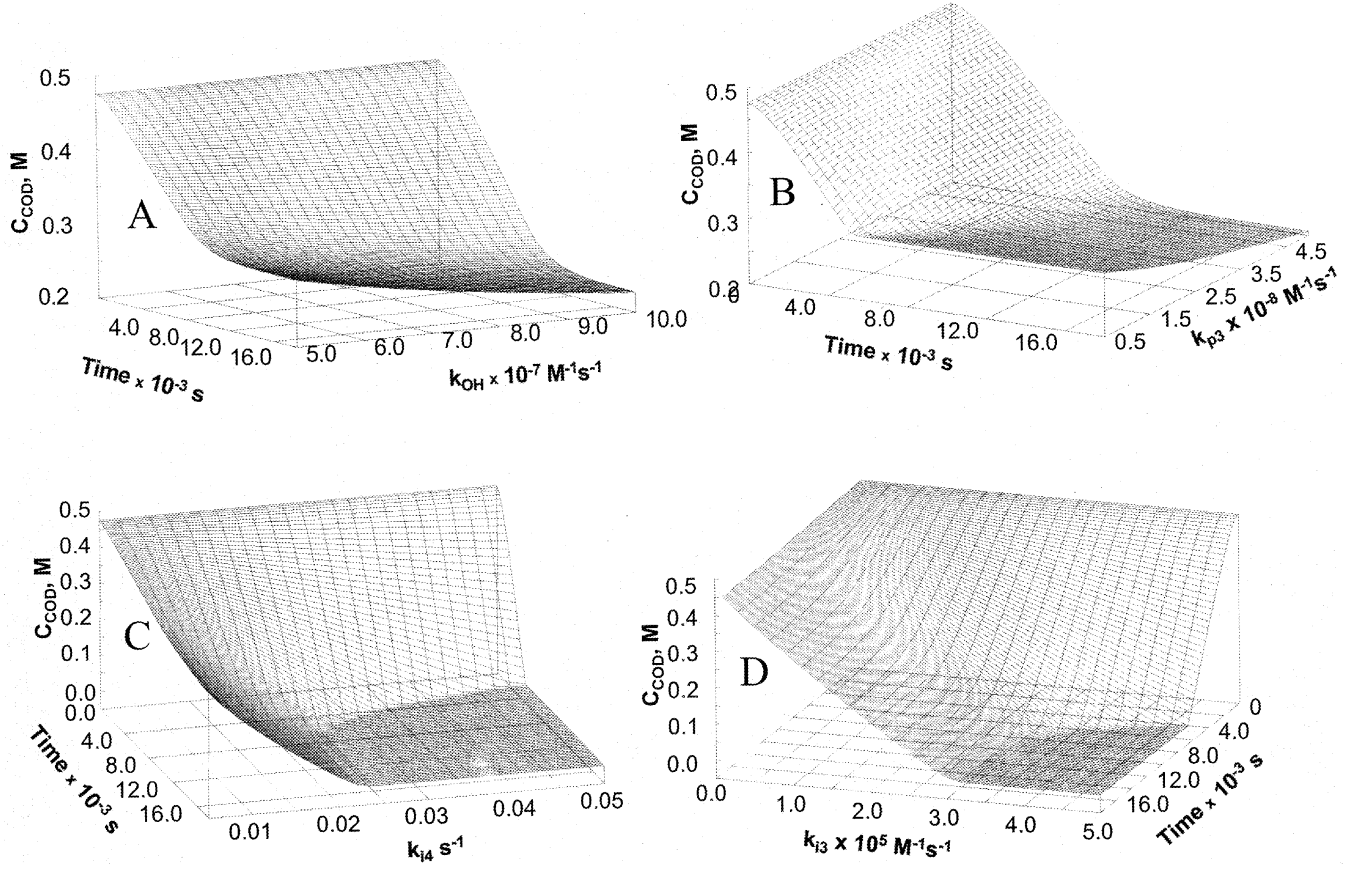

Fig. 5. Fe(III)/H_2O_2 treatment of fermentation table olive brines. Computed evolution of COD remaining concentration with time. Conditions: $pH_o = 3.5$; $T = 298$ K, $C_{H_2O_2} = 1.0$ M; $C_{Fe(III)} = 0.03$ M; $C_{COD_o} = 15\,g\,l^{-1}$. (A) Influence of k_{OH}. (B) Influence of k_{p3}. (C) Influence of k_{i4}. (D) Influence of k_{i3}.

for the aforementioned interval of k_{i4}. As expected, this step is crucial for the propagation of the radical chain, and hence, its value notoriously influences the COD removal profile, specially for values between 0.005 and 0.025 s^{-1}.

3.5.5. Kinetic constant for hydrogen peroxide decomposition, k_{ineff}

Similarly to the previous case, the ineffective decomposition of H_2O_2 leading to species other than oxidising molecules exerts a significant influence on the COD degradation rate. In Fig. 6 (A) and (B) the remaining concentrations of COD and H_2O_2 with time are plotted as a function of k_{ineff}. Obviously, both concentration profiles have opposite trends.

3.5.6. Kinetic constant for hydrogen peroxide decomposition by Fe(III), k_{i3}

Logically, the effective decomposition of H_2O_2 to initiate the radical mechanism leads to a higher COD elimination from the media. In Fig. 5 (D) it is shown the effect of this parameter in the range 1 to 5×10^{-5} M^{-1} s^{-1}. For values of k_{i3} above 5×10^{-5} the positive influence

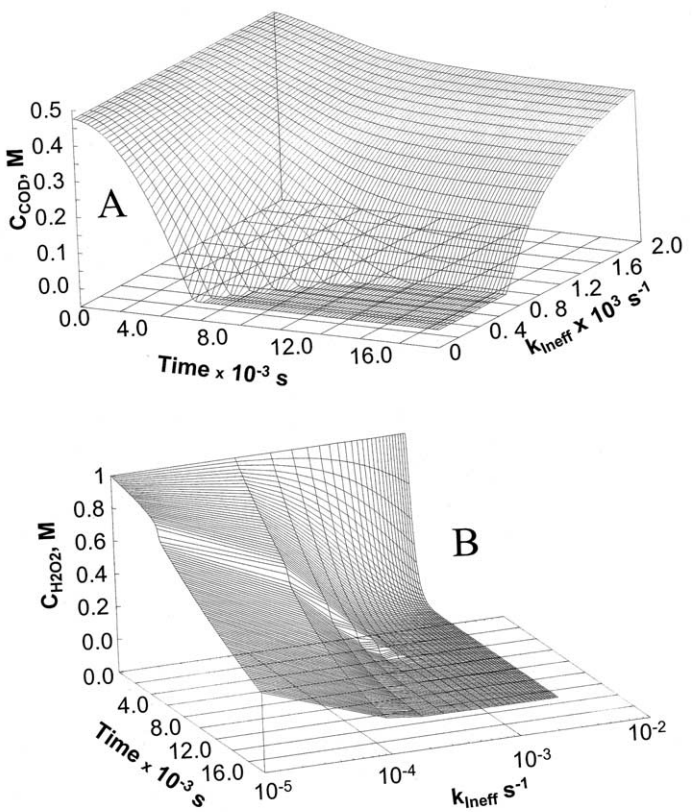

Fig. 6. Fe(III)/H_2O_2 treatment of fermentation table olive brines. Conditions: pH_o = 3.5; T = 298 K, $C_{H_2O_2}$ = 1.0 M; $C_{Fe(III)}$ = 0.03 M; C_{COD_o} = 15 $g\,l^{-1}$. Influence of k_{ineff}. (A) Computed evolution of COD remaining concentration with time. (B) Computed evolution of H_2O_2 remaining concentration with time.

was less pronounced. Hydrogen peroxide consumption was not affected by this parameter, therefore, in the proposed mechanism, at the conditions used, H_2O_2 disappearance through reaction k_{ineff} plays a more important role than the catalytic decomposition by Fe(III).

3.5.7. Kinetic constant for hydrogen peroxide decomposition by Fe(II), k_{i2}

This parameter had no effect on the mechanism for values in the range 1 to $10^3\,M^{-1}\,s^{-1}$. Typical values in organic free water goes from 50 to $100\,M^{-1}\,s^{-1}$.

3.5.8. Kinetic constant Fe(III) by organic radicals, k_{r3}

This rate constant was tested for values in the range 5×10^{-4} to $5 \times 10^{-5}\,M^{-1}\,s^{-1}$. Fig. 7 (A) shows the simulation results obtained when varying this parameter in the aforementioned interval. As observed from this figure, an increase of k_{r3} leads to similar COD removal rates at the beginning of the process, nevertheless, the final conversion achieved diminished as this kinetic constant was increased. At the sight of these results, this reaction

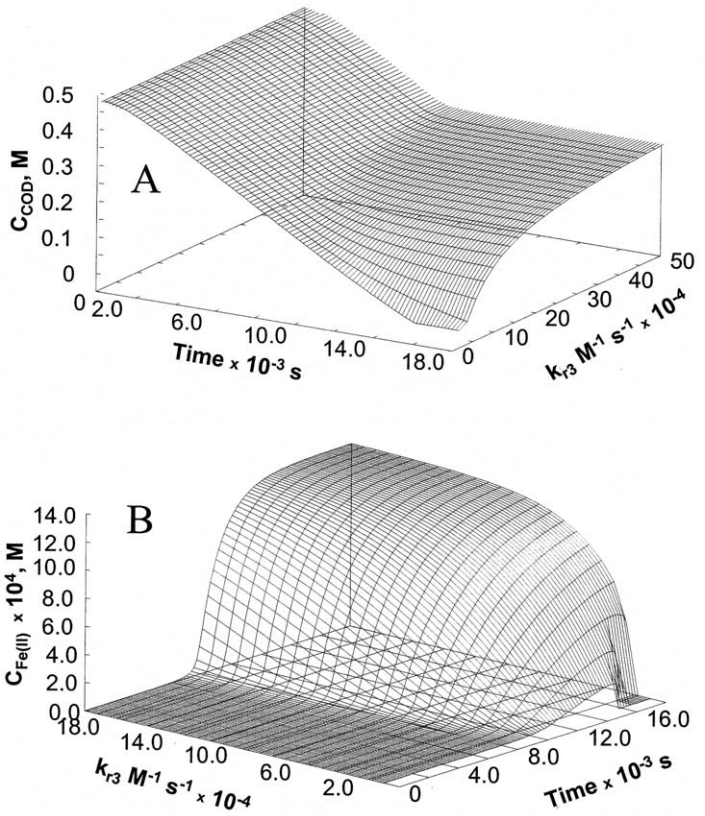

Fig. 7. Fe(III)/H_2O_2 treatment of fermentation table olive brines. Conditions: $pH_o = 3.5$; $T = 298\,K$, $C_{H_2O_2} = 1.0\,M$; $C_{Fe(III)} = 0.03\,M$; $C_{COD_o} = 15\,g\,l^{-1}$. Influence of k_{r3}. (A) Computed evolution of COD remaining concentration with time. (B) Computed evolution of Fe(II) concentration with time.

seems to be the main responsible of the Fe(II) accumulation in the media (see Fig. 7 (B)), inhibiting the chain reaction by scavenging the species $COD^{\bullet}$, of paramount importance to propagate the mechanism.

3.6. Aerobic biodegradation modelling

Modelling of aerobic biodegradation experiments was accomplished by considering the generalized Monod equation given by:

$$\mu = k_{obs}\frac{S}{S + K_{Sobs}} \tag{22}$$

where

$$k_{obs} = \mu_{max}\left[1 - \frac{C_i}{C_i^*}\right]^n \tag{23}$$

$$K_{Sobs} = K_S\left[1 - \frac{C_i}{C_i^*}\right]^m \tag{24}$$

μ and μ_{max} are the specific growth rate and the maximum specific growth rate, respectively, K_S the substrate concentration leading to a value of μ half of the μ_{max}, S is any parameter representing the limiting substrate in the process (i.e. BOD, COD, TC, etc) and C_i any species inhibiting the biodegradation (i.e. substrate, biomass, reaction products, etc.), the asterisk indicates the critical concentration above which no biodegradation occurs.

Since experiments were carried out under no inhibitory conditions and, normally $K_s \ll S$, Monod equation finally yields:

$$\mu = \frac{1}{X}\frac{dX}{dt} = \mu_{max} \tag{25}$$

where X refers to volatile suspended solid concentration (VSS).

In this study, the value of the biodegradable COD fraction (difference between actual COD and COD at infinite time) was adopted as the limiting substrate (COD_B). Additionally, the heterotrophic yield coefficient is defined according to:

$$Y_{VSS/COD_B} = \frac{VSS - VSS_o}{COD_{B_o} - COD_B} \tag{26}$$

Thus, by considering Eqs (25) and (26) the following expression can be deduced:

$$\ln\left[\frac{Y_{VSS/COD_B}(COD_{B_o} - COD_B) + VSS_o}{VSS_o}\right] = \mu_{max}\, t \tag{27}$$

If Eq. (27) applies, a plot of the left member of this equation against time should yield a straight line, the slope being the maximum specific growth rate. Figs. 8 and 9 shows the aforementioned representation for experiments carried out under a wide range of operating conditions. An acceptable consistency on the value of μ_{max} was obtained for experiments completed at similar pH (≈7) and temperature (≈20 °C) $\mu_{max} = 0.03\,h^{-1}$, this value is

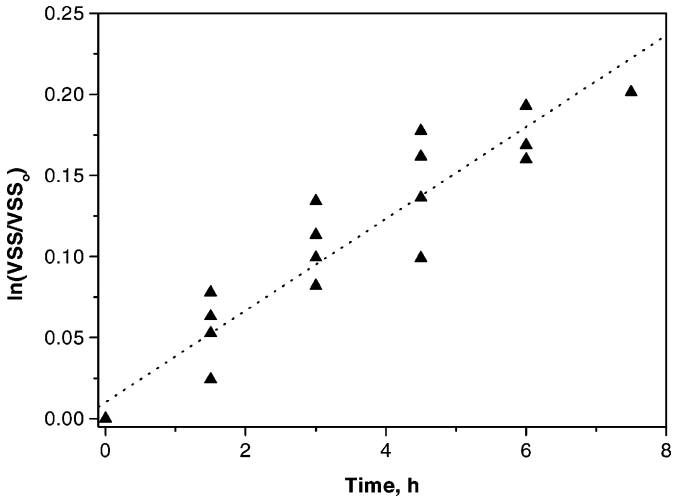

Fig. 8. Aerobic biological treatment of fermentation table olive brines after chemical pre-oxidation. Validation of Monod kinetics, Eq. (25). Conditions: $pH_o = 7.0$; $T = 293\,K$, $VSS_o/COD_o = 0.75–2.1$; $C_{COD_o} = 15\,g\,l^{-1}$ (average value).

comparable to other reported values for the aerobic biodegradation of analogous effluents after a pre-treatment by wet air oxidation [31].

Experiments conducted at different temperatures allowed for the determination of the apparent activation energy of the process. Thus, the following equation was obtained which related μ_{max} with temperature: $\mu_{max} = 9.02 \exp(-13786/RT)$. The low activation energy

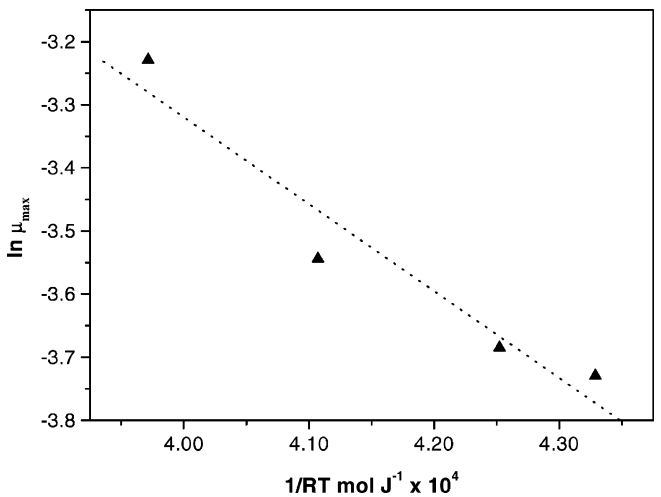

Fig. 9. Aerobic biological treatment of fermentation table olive brines after chemical pre-oxidation. Arrhenius plot. Conditions: $pH_o = 7.0$; $VSS_o/COD_o = 0.75–2.1$; $C_{COD_o} = 15\,g\,l^{-1}$ (average value).

found 13.8 kJ mol^{-1} has also been reported previously for the treatment of effluents from olive oil mills and table olive manufacturing industries by activated sludge [31,32].

4. Conclusions

In the past and recent literature, there is a lack of proposal and validation of kinetic mechanisms in real effluents treatment. In this paper, given the importance of modelization for design and control purposes, a semi-empirical model for the treatment of brines by Fenton's reagent has been presented. The model does a good job when simulating the profiles of the main species present in the aqueous matrix, i.e. COD and H_2O_2. Also, the mechanism of reactions predicts the positive effect of oxygen in the media and gives an approximation of the most important stages occurring in the liquid. Depending on reaction conditions, a shift in the rate of hydrogen peroxide decomposition is experimentally found. According to the proposed model, this fact may be explained if the semi-empirical constant k_{ineff} changes as the initial ferric iron used changes. The correlation between both parameters (not given in this paper) should be investigated in future works. Additionally, a simple Monod expression can be used to model the aerobic biodegradation of the effluent obtained after the chemical oxidation pre-treatment. Kinetic parameters calculated from this model are comparable to those reported in previous works dealing with similar wastewaters.

Acknowledgements

This work has been supported by the Junta de Extremadura opf Spain and Social Europena Funds (Project IPR00A002).

References

[1] F.J. Rivas, F.J. Beltran, O. Gimeno, P. Alvarez, J. Haz. Mater. B, 2000, in press.
[2] R.J. Bidga, Chem. Eng. Prog. December (1995) 62.
[3] R.J. Bidga, Environ. Technol. May/June (1996) 34.
[4] F.J. Rivas, F. Beltran, J. Frades, O. Gimeno, J. Agric. Food Chem. 49 (2001) 1873.
[5] C. Walling, Acc. Chem. Res. 8 (1975) 125.
[6] S.H. Bossmann, E. Oliveros, S. Göb, S. Siegwart, E. Dahlen, L. Payawan, M. Straub, M. Wörner, J. Phys. Chem. A 102 (1998) 5542.
[7] R. Chen, J. Pignatello, Environ. Sci. Technol. 31 (1997) 2399.
[8] F.J. Rivas, F.J. Beltran, J. Frades, P. Buxeda, Water Res. 35 (2001) 387.
[9] P.A. MacFaul, D.M. Wayner, K.U. Ingold, Acc. Chem. Res. 31 (1998) 159.
[10] I. Yamazaki, L.H. Piette, J. Am. Chem. Soc. 113 (1991) 7588.
[11] C. Walling, Acc. Chem. Res. 31 (1998) 155.
[12] D.T. Sawyer, A. Sobkowiak, T. Matsushita, Acc. Chem. Res. 29 (1996) 409.
[13] C. Walling, K. Amarnath, J. Am. Chem. Soc. 104 (1982) 1185.
[14] M. Fukushima, K. Tatsumi, Coll. Surf. A: Physicochem. Eng. Aspects 155 (1999) 249.
[15] B. Voelker, B. Sulzberger, Environ. Sci. Technol. 30 (1996) 1106.
[16] G. Tachiev, J. Roth, R. Bowers, Int. J. Chem. Kinet. 32 (2000) 24.
[17] I.A. Salem, M. El-Maazawi, A. Zaki, Int. J. Chem. Kinet. 32 (2000) 643.
[18] S. Rahhal, H. Richter, J. Am. Chem. Soc. 110 (1988) 3127.

[19] R. Watts, M. Foget, S. Kong, M. Teel, J. Haz. Mater. B69 (1999) 229.
[20] J. Kiwi, A. Lopez, V. Nadtochenko, Environ. Sci. Technol. 34 (2000) 2162.
[21] V. Nadtochenko, J. Kiwi, Environ. Sci. Technol. 32 (1998) 3273.
[22] F.J. Rivas, S.T. Kolaczkowski, F.J. Beltrán, D.B. McLurgh, Chem. Eng. Sci. 53 (1998) 2575.
[23] B. Utset, G. Garcia, J. Casado, X. Domenech, J. Peral, Chemosphere 41 (2000) 1187.
[24] H. Tung, C. Kang, D.T. Sawyer, J. Am. Chem. Soc. 114 (1992) 3445.
[25] G.V. Buxton, C.L. Greenstock, W.P. Helman, A.B. Ross, J. Phys. Chem. Ref. Dat. 17 (1988) 513.
[26] P. Neta, R. Huie, A.B. Ross, J. Phys. Chem. Ref. Dat. 19 (1990) 413.
[27] C.M. Miller, R.L. Valentine, Water Res. 33 (1999) 2805.
[28] N. Kitajima, S. Fukuzumi, Y. Ono, J. Phys. Chem. 82 (1978) 1505.
[29] P. Mendes, D.B. Kell, Bioinformatics 14 (1998) 869.
[30] T. Bäck, H.P. Schwefel, Evolutionary Comput. 1 (1993) 1.
[31] F.J. Rivas, F.J. Beltrán, O. Gimeno, Chem. Eng. Technol. 23 (2000) 177.
[32] F.J. Rivas, F.J. Beltrán, O. Gimeno, P. Alvarez, J. Environ. Eng. 127 (2001) 611.